

FLOW TRANSITIONS IN THE WAKE OF A STREAMWISE-ROTATING SPHERE

C.J. Pregalato, M.C. Thompson and K. Hourigan
Fluids Laboratory for Aeronautical and Industrial Research (FLAIR)
Department of Mechanical Engineering, Monash University, Clayton VIC 3800, Australia
Email: craig.pregalato@eng.monash.edu.au

ABSTRACT

The flow past a streamwise-rotating sphere is investigated numerically for Reynolds numbers (based on sphere diameter) in the range $10 < Re < 500$, and dimensionless rotation speeds of $0 < \Omega < 0.25$. In particular, we focus on the influence of sphere rotation rates on the transition (or critical) Reynolds numbers. It is found that the transition to three-dimensionality occurs at a Reynolds number, Re_1 , which is highly dependent on the rotation rate. Furthermore, the transition to unsteadiness, which is characterized by the presence of hairpin vortex shedding, occurs at higher Reynolds numbers for intermediate rotation rates. An interesting characteristic of the flow is the appearance of “frozen” vortex structures, which simply rotate in the wake without variation in shape or strength. These vortex structures are not observed for a stationary sphere.

INTRODUCTION

The flow over a rotating sphere is of great interest in many engineering applications, from particle transport and sedimentation processes to sports and the trajectories of spinning balls. In either case, it is extremely useful to know how rotation affects the motion of the object, which in turn requires knowledge of the forces acting on the body. For a non-rotating sphere, the transitions to asymmetry (three-dimensionality) and unsteadiness are well documented. For example, Natarajan and Acrivos (1993) report a value of $Re_1 = 210$ and $Re_2 = 277.5$ from their linear stability analysis. However, their value of Re_2 is not entirely accurate because the base flow used for the analysis was axisymmetric. Nonetheless, these results are in agreement with the values of $Re_1 = 212$ and $Re_2 = 272$ obtained by Thompson *et al.* (2001) who modeled the transitions by constructing Landau models and determining the coefficients. It should be noted that the majority of research concerning rotating spheres has focused on rotation about the axis transverse to the fluid flow. These studies have focused primarily on the drag and lift forces experienced by the sphere (see, for example, Barkla & Auchterlonie (1971), Tsuji *et al.* (1985), Oesterle & Bui Dinh (1999), Kurose & Komori (1999)). However, very few studies have dealt with spheres rotating about the *streamwise* axis. Schlichting (1979) points out that when Ω is increased, the line of laminar separation moves upstream, meaning that the centrifugal forces acting on the fluid particles rotating with the sphere in its boundary layer have the same effect as an additional pressure gradient directed towards the plane of the equator. Kim and Choi (2002) numerically simulated the laminar flow past a streamwise-rotating sphere at Reynolds numbers of $Re = 100, 250$ and 300 and sphere rotation rates of $0 \leq \Omega \leq 1$. Along with the usual two-tail wake and hairpin vortex shedding for stationary spheres, they found that with streamwise rotation a “frozen” state of the flow could be observed. This frozen state was detected at $\Omega = 0.5$ and 0.6 for $Re = 300$, and at $\Omega = 0.1$ and 0.3 for $Re = 250$. Furthermore, at $Re = 250$, the flow became unsteady for all the rotational speeds investigated. However, no attempt was made to investigate the effect of different rotation rates on the wake transitions, which is the main focus of this study. Some of the results reported here, as well as additional data concerning the effect of *non-streamwise* rotation rates, were first presented in Pregalato *et al.* (2001).

NUMERICAL METHOD

The flow past a rotating sphere is investigated in the Reynolds number range $10 < Re < 500$, with rotation rates varying in the range $0 < \Omega < 0.25$. This particular parameter regime was chosen because the flow phenomena of interest, namely the transitions to asymmetry and three-dimensionality, are well documented in this regime. Furthermore, many results (such as lift, drag and Strouhal number) are available for a stationary sphere ($\Omega = 0$) that provide a basis from which to compare the present results.

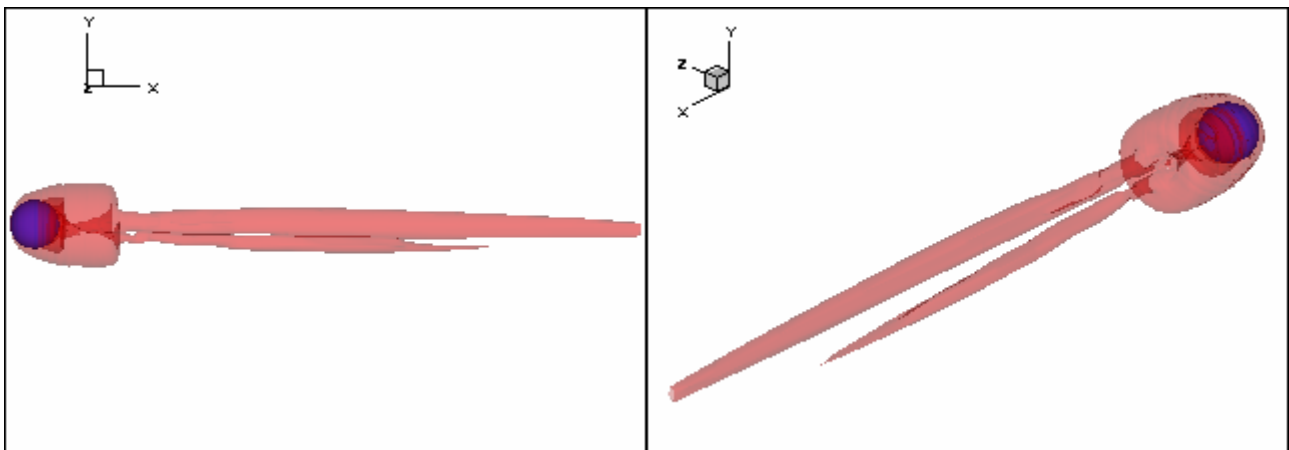


Figure 1. Vortex structures in the wake of a streamwise rotating sphere: $Re = 260, \Omega = 0.05$.

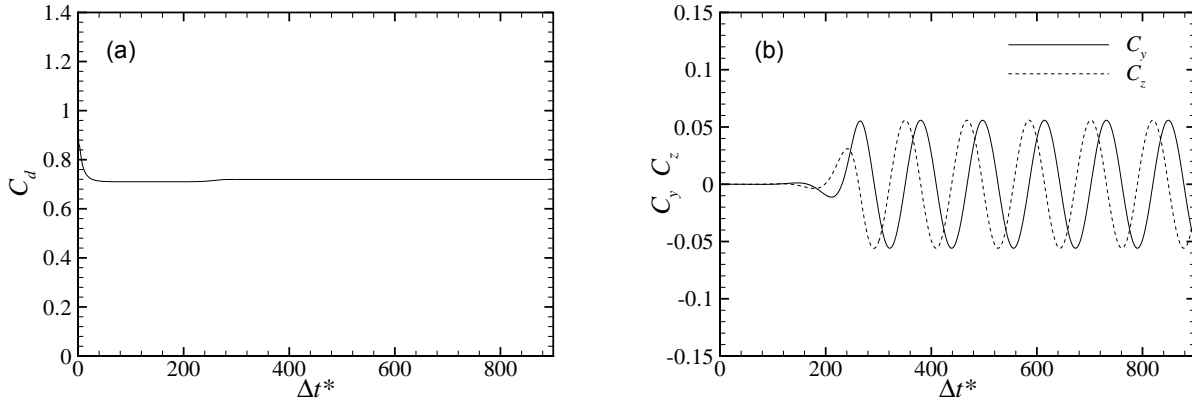


Figure 2. Force coefficient history for $Re = 240$, $\Omega = 0.15$: (a) C_D time history; (b) C_y and C_z time histories.

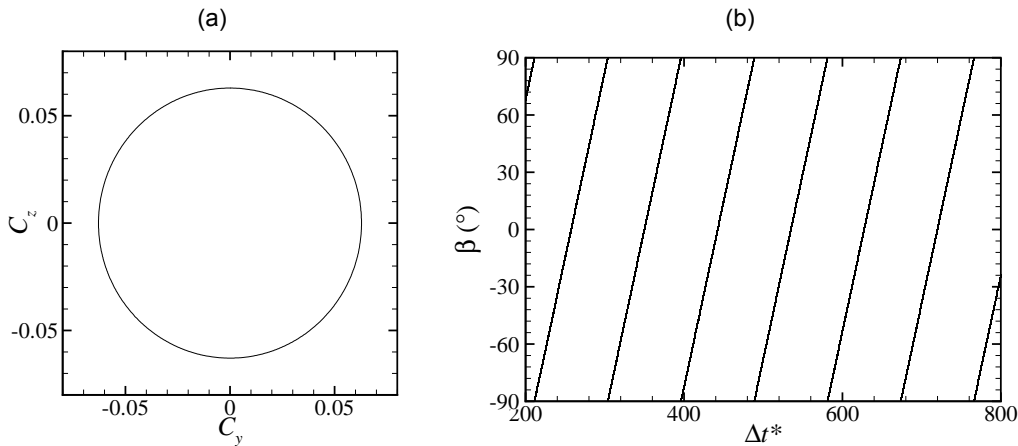


Figure 3. $Re = 260$, $\Omega = 0.10$: (a) C_y - C_z phase plot; (b) history of angle of lift coefficient, β .

A three-dimensional spectral element/spectral method is used to simulate the viscous, incompressible flow past a streamwise-rotating sphere. Eighth-order tensor-product Lagrange polynomials were used as the interpolating functions in each element. A detailed mesh-independence study was performed and is described in Pregalato *et al.* (2001).

The fluid forces acting on the sphere were computed according to the relation

$$F_\alpha = -\int_S p e_\alpha \cdot n \, dS + \int_S n \cdot \tau \cdot e_\alpha \, dS,$$

where α denotes the spatial coordinate of interest, i.e. x , y or z . When normalized by $1/8\rho\pi U^2 d^2$, the force coefficients C_x (or C_D), C_y and C_z are obtained, known as the drag, lateral and side force coefficients respectively. Similarly, the lift coefficient C_L is defined as the magnitude of the lateral and side force coefficients, i.e. $C_L^2 = C_y^2 + C_z^2$.

The (dimensionless) sphere rotation rate is defined as

$$\Omega = \frac{\Omega^* d}{2U},$$

where Ω^* is the (streamwise) angular velocity of the sphere in rad/s. Vortex structures in the wake of the sphere are visualized by the method of Jeong and Hussain (1995).

RESULTS

Given the amount of studies concerning rotating spheres, it is somewhat surprising to note that there is a significant lack of data concerning a *streamwise*-rotating sphere. As outlined in the Introduction, previous research regarding spheres rotating about the streamwise axis concentrated on the relationship between the rotation speeds and the fluid forces acting on the sphere. Although Kim and Choi (2002) investigated the effect of streamwise rotation on the drag, lift and vortical structure characteristics for select Reynolds numbers, no attempt has been made as yet to describe the relationship between rotation rates and the wake transitions over a large range of Reynolds numbers, which is the focus of the present study.

Different views of the vortex structures in the wake of the rotating sphere are shown in Figure 1 for a streamwise rotation rate of $\Omega = 0.05$ and for $Re = 260$. At this Reynolds number, the wake has become asymmetric, and exhibits a two-tail structure well documented in experiments. However, in this case the wake is no longer planar-symmetric, and the two tails have become skewed with respect to the streamwise axis. Furthermore, the strength of one tail has become greater

than the other. Due to the no-slip condition on the surface of the sphere, it is evident that fluid passing over the surface of the sphere attains the strong azimuthal velocity of the sphere. This serves to increase the strength of the streamwise vorticity that acts in the same direction as the rotation of the sphere, and annihilates the streamwise vorticity that is in the opposite direction of rotation. This leads to two counter-rotating vortices of dissimilar strength, and causes them to migrate away from the flow centreline due to their mutual vortical interaction. However, for this particular case, the flow is unsteady, although vortex shedding is not observed. This represents an example of a “frozen” flow, a term first coined by Kim and Choi (2002) to characterize a flow in which the vortex structures, although maintaining the same shape and strength for all time, rotate about the streamwise axis at an angular velocity different to that of the sphere. This is evident in the time histories of the fluid force coefficients shown in Figure 2 and discussed in the next section.

If the rotation rate is low enough ($\Omega < 0.15$), as in Figure 1, then a two-tail wake structure is observed. However, for higher rotation rates, the intensity of the stronger vortex completely overwhelms the weaker vortex and a single tail is observed immediately adjacent to the wake centreline. Figure 2 depicts the time variation of the drag, lateral and side force coefficients for $Re = 240$ and $\Omega = 0.15$. The simulation was initialized with the corresponding solution for a stationary sphere at the same Reynolds number. The drag coefficient remains constant in time, whereas the lateral and side force coefficients are sinusoidal with a frequency of $St_F = 0.017$. Note that St_F is a frequency based on the “frozen” state of the flow and is different to the Strouhal frequency, St , associated with vortex shedding. Since the time-averaged lateral and side forces are zero, the vortical structure in the wake simply rotates in a frozen state without temporal variation of its shape or strength. This previously unobserved flow phenomenon was first reported by Kim and Choi (2002) and the present results provide the first independent verification of such a flow feature for the spinning sphere.

Further information regarding the net lift may be obtained from the $C_Y - C_Z$ phase plot. An example is shown in Figure 3a for a typical frozen flow, in this case at a Reynolds number of $Re = 260$ for a rotation rate of $\Omega = 0.10$. Note that the net lift C_L is the distance from the origin to the curve. Because the curve is a perfect circle, it is evident that the net lift is constant, even though the time-averaged lateral and side force coefficients are zero. Also, in general, the rotation rate of the vortical structures is different to that of the sphere. This may be observed by recording the time history of the lift angle β , which is plotted in Figure 3b. The angular velocity of the frozen vortical structures in the wake is determined by the slope of β , i.e. $\Omega_L \equiv$ angular velocity of frozen vortical structures $= d\beta/dt$ in rad/s. In this example, the frozen vortex structures are rotating at a dimensionless angular velocity of $\Omega_F = 0.034$, whereas the sphere is rotating at $\Omega = 0.10$. Continuing with this Reynolds number of $Re = 260$, we find that increasing the rotation rate serves to increase the rotation rate of the frozen vortical structures, in an almost one: one correspondence. In other words, doubling the rotation rate of the sphere will double the rotation rate of the frozen vortical structures as well, assuming that the flow is still frozen at these higher angular velocities.

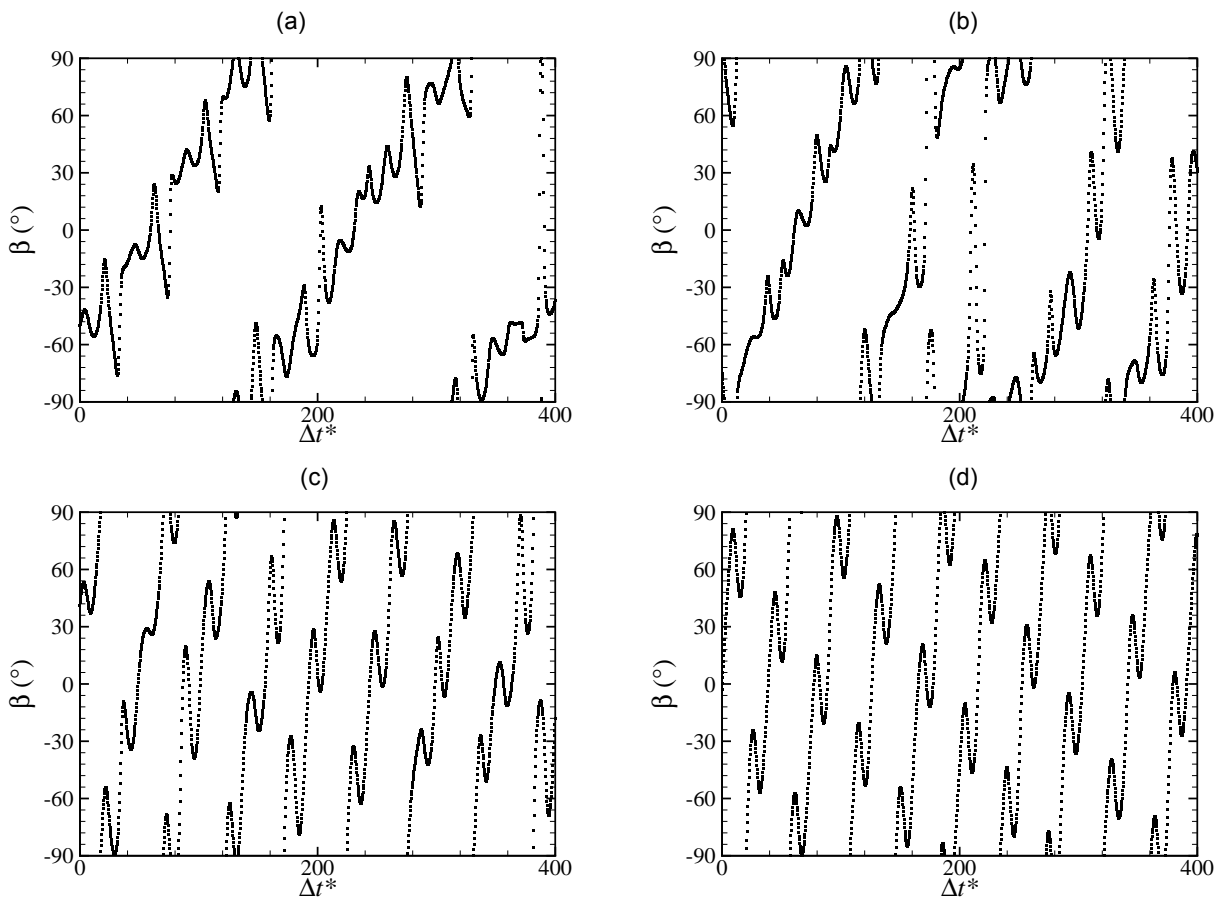


Figure 4. Time histories of β for $Re = 400$: (a) $\Omega = 0.05$; (b) $\Omega = 0.10$; (c) $\Omega = 0.20$; (d) $\Omega = 0.25$.

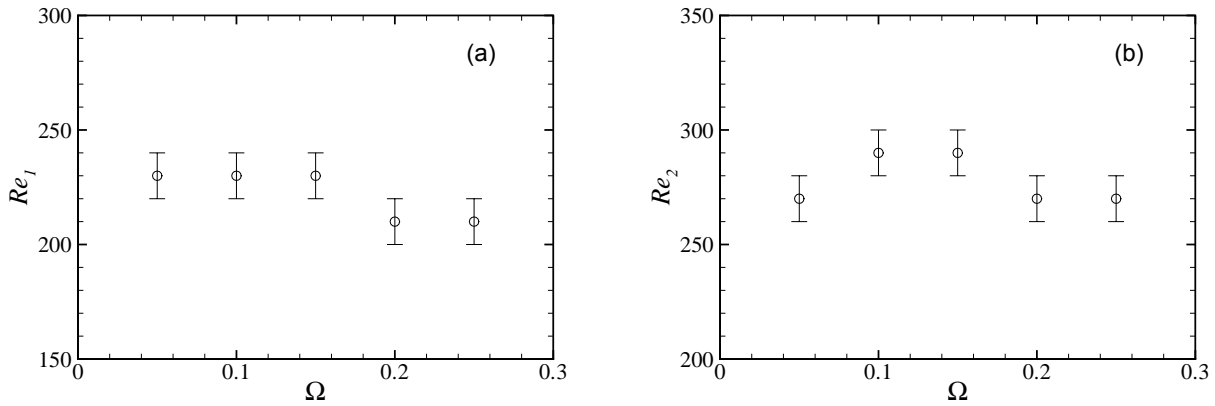


Figure 5. Critical Reynolds numbers as a function of sphere rotation rate: (a) transition to asymmetry; (b) transition to unsteadiness.

At a Reynolds number of $Re = 400$, for all rotation rates investigated (including zero rotation), the flow field is unsteady, asymmetric and well within the vortex shedding regime. Figure 4 shows typical time histories of the angle of lift β for different rotation rates. At low rotation rates, it is clear that vortices are being shed azimuthally in an aperiodic fashion, and hence Ω_L is not constant. However, as the rotation rate increases, the flow becomes more organized, and the vortex structures are shed with a relatively constant angular velocity. It appears that increasing the rotation rate further will lead to the appearance of frozen vortical structures at these higher Reynolds numbers, which is a topic of further study. Note that for all rotation rates investigated, there is no preferred angle of vortex orientation.

The transition to asymmetry, which occurs at a critical Reynolds number Re_1 , is shown in Figure 5a. Also illustrated is the second transition to unsteadiness (Figure 5b), which occurs at a critical Reynolds number Re_2 . Note that Re_2 in this sense denotes the Reynolds number at which vortex shedding first occurs and not necessarily the onset of time-dependence (since the frozen fields observed in Figure 2 are time-dependent although vortex shedding is not observed). This makes it somewhat easier to compare the present results concerning the wake transitions to that of a stationary sphere. It is apparent that for rotation rates less than $\Omega = 0.2$, the flow becomes asymmetric at a critical Reynolds number in the range $220 < Re_1 < 240$. For $\Omega \geq 0.2$, the transition occurs in the Reynolds number range $200 < Re_1 < 220$. For a stationary sphere, this transition occurs at a Reynolds number of $Re_1 \approx 212$. Furthermore, vortex shedding first occurs in the range $260 < Re_2 < 280$ for rotation rates of $\Omega = 0.05, 0.20$ and 0.25 , which is close to the value of $Re_2 \approx 272$ for a stationary sphere. However, for rotation rates of $\Omega = 0.10$ and 0.15 , the transition occurs in the Reynolds number range $280 < Re_2 < 300$.

CONCLUSION

The flow past a streamwise-rotating sphere was investigated numerically using a three-dimensional spectral element/Fourier method developed for axisymmetric geometries. Dimensionless sphere rotation rates of $0.05 < \Omega < 0.25$ were investigated for the first time in the Reynolds number range $10 < Re < 500$. It was discovered that in general, depending on the magnitude of streamwise rotation, the transition to asymmetry was delayed and the transition to unsteadiness occurred in the range of Reynolds numbers in which unsteadiness for a stationary sphere also occurs. Furthermore, the vortex structures in the wake are greatly affected by the rate of rotation.

REFERENCES

- Barkla, H.M. & Auchterlonie, L.J. 1971 The Magnus or Robins effect on rotating spheres. *J. Fluid Mech.* **47**, 437-447.
- Jeong, J. & Hussain, F. 1995 On the identification of a vortex. *J. Fluid Mech.* **285**, 69-94.
- Kim, D. & Choi, H. 2002 Laminar flow past a sphere rotating in the streamwise direction. *J. Fluid Mech.* (to appear).
- Kurose, R. & Komori, S. 1999 Drag and lift forces on a rotating sphere in a linear shear flow. *J. Fluid Mech.* **384**, 183-206.
- Natarajan, R. & Acrivos, A. 1993 The instability of the steady flow past spheres and disks. *J. Fluid Mech.* **254**, 323-344.
- Oesterle, B. & Bui Dinh, T. 1999 Experiments on the lift of a spinning sphere in a range of intermediate Reynolds numbers. *Exp. Fluids* **25**, 16-22.
- Pregalato, C.J., Thompson, M.C. & Hourigan, K. 2001 *14th Australasian Fluid Mech. Conf.* (Ed. B. Dally) Adelaide, Dec 15-18.
- Schlichting, H. 1979 *Boundary Layer Theory*. 7th edn. McGraw-Hill.
- Thompson, M.C., Leweke, T. & Provansal, M. 2001 Kinematics and dynamics of sphere wake transition. *J. Fluids Struct.* **15**, no. 3-4, 575-585.
- Tsuji, Y., Morikawa, Y. & Mizuno, O. 1985 Experimental measurement of the Magnus force on a rotating sphere at low Reynolds numbers. *Trans. ASME J. Fluids Eng.* **107**, 484-488.